hv photonics

IMPACT FACTOR 2.536

CITESCORE 2.3

Article

Decoherence of Higher Order Orbital Angular Momentum Entangled State in Non-Kolmogorov Turbulence

Xiang Yan, Pengfei Zhang, Boying Wu and Jinghui Zhang

Topic

Applications of Photonics, Laser, Plasma and Radiation Physics

Edited by

Prof. Dr. Viorel-Puiu Paun, Prof. Dr. Eugen Radu and Prof. Dr. Maricel Agop

MDPI

https://doi.org/10.3390/photonics9110808

photonics

MDPI

Article

Decoherence of Higher Order Orbital Angular Momentum Entangled State in Non-Kolmogorov Turbulence

Xiang Yan [1], Pengfei Zhang [2], Boying Wu [1,*] and Jinghui Zhang [2]

[1] School of Physics and Electronic Information Engineering, Hubei Engineering University, Xiaogan 432000, China
[2] Key Laboratory of Atmospheric Composition and Optical Radiation, Anhui Institute of Optics and Fine Mechanics, Chinese Academy of Sciences, Hefei 230031, China
* Correspondence: wuboying4768863@126.com

Abstract: The decay of OAM entanglement in non-Kolmogorov turbulence has been numerically evaluated. In this work, we explore the evolution of OAM entanglement with higher-order OAM mode in the weak scintillation regime. In particular, the results of the numerical evaluation show that the OAM entanglement state with higher value of the azimuthal mode and larger radial quantum number survives over a longer distance. Meanwhile, the beam parameters and turbulence parameters usually have significant influences on OAM entanglement. In addition, it is demonstrated that the effect of turbulence on the OAM entanglement is the most serious when the generalized exponent is around 3.07.

Keywords: orbital angular momentum; entangled state; higher-order mode; non-Kolmogorov turbulence

Citation: Yan, X.; Zhang, P.; Wu, B.; Zhang, J. Decoherence of Higher Order Orbital Angular Momentum Entangled State in Non-Kolmogorov Turbulence. *Photonics* **2022**, *9*, 808. https://doi.org/10.3390/photonics9110808

Received: 25 August 2022
Accepted: 24 October 2022
Published: 27 October 2022

1. Introduction

Orbital angular momentum (OAM) photons have gained more and more attention in recent years. The orbital angular momentum (OAM) eigenstates of photons form an infinite-dimensional system, providing larger storage capacity and a number of potential benefits for quantum information purposes [1–5], which make them promising candidates for higher dimensional quantum key distribution [6].

Quantum entanglement is an essential physical resource, which can be applied significantly in the field of quantum information processing [7,8] but is highly fragile to the environment [9]. Recently, an enormous number of theoretical and experimental studies have been devoted to the turbulence-induced decay of OAM entanglement [9–21]. Nonetheless, it is still difficult to describe the behavior of OAM photons in turbulence. It is known that OAM-entangled photonic states are encoded in finite-dimensional Hilbert spaces. While OAM-entangled photons go through atmospheric turbulence, the scintillation process distorts the photons' wave fronts and makes OAM modes spread throughout the entire Hilbert space [22]. In practice, however, only the information of the output states contained in the finite-dimensional encoding subspace can be extracted. As a consequence, it is essential to truncate the Hilbert space and calculate the truncated density matrix for predicting OAM entanglement evolution. The truncated density matrix can obtain the scattering to density matrix elements from outside the subspace, but the effect of backward scattering from the outside subspace to elements in the subspace is always lost [20]. However, when the coupling of states between inside the encoding subspace and outside is strong, the truncation of the Hilbert space unavoidably leads to a decay of the output state's norm [23], and the backward scattering is particularly important to higher-order OAM modes [24]. Moreover, most previous theoretical studies on the effects of atmospheric turbulence on OAM entanglement have always considered the entangled OAM states with a zero radial index [14–20], but the entanglement decoherence of OAM photons with non-zero radial index has seldom been mentioned.

In the present contribution, the OAM-entangled two-photon state's propagation through a non-Kolmogorov turbulent atmosphere has been numerically evaluated. We consider that the evolution of the OAM entanglement is in the weak scintillation regime. Therefore, the turbulence-caused intensity scintillation is ignored. Here, we significantly focus on the evolution of OAM entanglement with higher-order OAM mode in turbulence when the backward scattering is taken into account. In addition, Wootter's concurrence is introduced to quantify the OAM entanglement [25]. The rest of the paper is organized as follows: In Section 2, the numerical procedure will be introduced, while the results of numerical evaluation and its analysis will be provided in Section 3. The discussion and conclusions are presented and provided in Section 4.

2. Numerical Procedure

The quantum communication system is presented in Figure 1. A pair of entangled photons are emitted by the source field. Initially, it is in a Bell state and can be expressed as

$$|\psi\rangle_{\text{in}} = \frac{1}{\sqrt{2}}(|\ell, p\rangle_{\text{A}}|-\ell, p\rangle_{\text{B}} + |-\ell, p\rangle_{\text{A}}|\ell, p\rangle_{\text{B}}), \tag{1}$$

where the footnotes A and B represent two different paths of photons, p is the radial quantum number, and ℓ is the azimuthal mode order of the Laguerre-Gaussian (LG) beam. In the cylindrical coordinates, a single photon LG mode can be expressed as [22].

$$\langle r\,|\ell\rangle = \frac{1}{\sqrt{2\pi}} R_{\ell,p}(r,z)\exp(i\ell\theta), \tag{2}$$

where $r^2 = x^2 + y^2$, and the parameter θ is the azimuthal angle. The LG function $R_{\ell,p}(r,z)$ in normalized cylindrical coordinates can be written as [26–28]

$$R_{\ell,p}(r,z) = \frac{A_{lp}}{w(\mathrm{z})}\left(\frac{\sqrt{2}r}{w(\mathrm{z})}\right)^{|\ell|} L_p^{|\ell|}\left(\frac{2r^2}{w^2(\mathrm{z})}\right)\exp\left(-\frac{r^2}{w^2(\mathrm{z})}\right)\exp\left\{\mathrm{i}(\ell+1)\tan^{-1}(z/z_R) - \frac{\mathrm{i}kr^2}{2z\left[1+(z_R/z)^2\right]}\right\}, \tag{3}$$

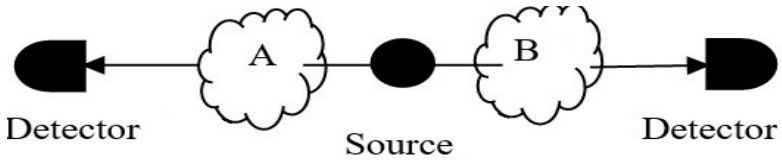

Figure 1. Sketch of the setup. A pair of entangled photons are generated by a source, and propagate along two weakly turbulent atmospheres which are labeled by A and B toward two detectors.

Here $A_{\ell p} = \left(\frac{p!2^{|\ell|}}{\pi(p+|\ell|)!}\right)^{1/2}$ is a normalization constant, the parameter $w = w_0\sqrt{1+(\mathrm{z}/\mathrm{z}_R)^2}$ is related to the propagation distance z and initial beam radius w_0, and the Rayleigh range $\mathrm{z}_R = kw_0^2/2$ is the waist radius of the Gaussian beam in the receiver plane. The Rayleigh range is correlated with the wavelength λ by the ratio $k = 2\pi/\lambda$ (the wave number), and $L_p^{|\ell|}(\cdot)$ represents the associated Laguerre polynomials.

As the photons travel through the turbulent atmosphere, OAM modes are distorted by the modulations of the random phase of the turbulent atmosphere, leading to the decay of OAM entanglement. Generally, the output density matrix ρ_{out} is used for determining the OAM entanglement after passing through turbulence [14,17,24], and

$$\rho_{\text{out}} = \sum_{mnm'n'} \rho_{m,n,m',n'}|\ell_m, \ell_{m'}\rangle_{\text{AB}}\langle\ell_{n'}, \ell_n|. \tag{4}$$

$\rho_{m,n,m',n'}$ is the density matrix element of output state [17,24], and

$$\rho_{m,n,m',n'} = \langle \ell_{m'}, \ell_m | \psi_I \rangle \langle \psi_I | \ell_n, \ell_{n'} \rangle, \tag{5}$$

where $|\ell_m\rangle(|\ell_{m'}\rangle)$ and $|\ell_n\rangle(|\ell_{n'}\rangle)$ are direct measurement states. The input state $|\psi\rangle_{in}$ propagating through the atmospheric turbulence changes into the state $|\psi_I\rangle$. In the weak turbulence regime, the impacts of the turbulent atmosphere on OAM photons are equivalent to phase errors in the transverse beam profile [22], leading to

$$\langle r|\psi_I\rangle = \frac{1}{\sqrt{2}} \left(\langle r|\ell\rangle_{\mathrm{A}} \langle r|-\ell\rangle_{\mathrm{B}} e^{\mathrm{i}(\phi_A(r)+\phi_B(r))} + \langle r|-\ell\rangle_{\mathrm{A}} \langle r|\ell\rangle_{\mathrm{B}} e^{\mathrm{i}(\phi'_A(r)+\phi'_B(r))} \right), \tag{6}$$

where the random perturbations $\phi_j(r)$ and $\phi'_j(r)$ (j= A, B) are induced by two weakly turbulent atmospheres.

Note that the scintillation process can make the OAM modes spread through the entire Hilbert space. To deal with an infinite-dimensional Hilbert space of output states upon detection, the truncated Hilbert space is necessary. In this paper, at first we extract the OAM information contained in the modes, which are $\pm\ell \pm 1$ and $\pm\ell$, and then project the transmitted state on encoding subspace $|\ell,\ell\rangle, |\ell,-\ell\rangle, |-\ell,\ell\rangle, |-\ell,-\ell\rangle$. Hilbert-space truncation does keep track of the scattering to density matrix elements that are inside the subspace, but the backward scattering from outside the subspace to elements in the encoding subspace is lost. Because OAM modes that are outside the subspace can also be scattered back to the encoding subspace due to scintillation, the backward scattering is very important for evaluating the evolution of OAM entanglement through turbulence. Considering the effect of backward scattering, the output density matrix ρ_{out} is readily found to be [24]

$$\begin{pmatrix} \rho_{11} & 0 & 0 & 0 \\ 0 & \rho_{22} & \rho_{23} & 0 \\ 0 & \rho_{32} & \rho_{33} & 0 \\ 0 & 0 & 0 & \rho_{44} \end{pmatrix}. \tag{7}$$

For $|\ell|$= 1, the matrix elements are described by

$$\rho_{11} = 4abc_1c_2 + 2ab, \tag{8}$$

$$\rho_{22} = c_1^2c_2^2 + 2a^2c_1c_2 + 2b^2c_1c_2 + a^2 + b^2, \tag{9}$$

$$\rho_{23} = c_1^2c_2^2 + 2a^2c_1c_2 + a^2, \tag{10}$$

$$\rho_{32} = \rho_{23}, \tag{11}$$

$$\rho_{33} = \rho_{22}, \tag{12}$$

$$\rho_{44} = \rho_{11}. \tag{13}$$

Otherwise

$$\rho_{11} = 2ab(2c_1c_2 + 2c_1c_3 + 1), \tag{14}$$

$$\rho_{22} = c_1^2(c_2 + c_3)^2 + \left(a^2 + b^2\right)(2c_1c_3 + 2c_1c_2 + 1), \tag{15}$$

$$\rho_{33} = 2c_1^2c_3(c_2 + c_3) + \left(a^2 + b^2\right)(3c_1c_3 + c_1c_2 + 1), \tag{16}$$

$$\rho_{44} = 2ab(c_1c_2 + 3c_1c_3 + 1), \tag{17}$$

$$\rho_{23} = c_1^2(c_2 + c_3)^2 + a^2(2c_1c_3 + 2c_1c_2) + a^2, \tag{18}$$

$$\rho_{32} = c_1^2(c_2 + c_3)^2 + a^2(2c_1c_3 + 2c_1c_2) + a^2, \tag{19}$$

where a is the survival amplitude with $|\Delta\ell| = 0$ [14], b is crosstalk amplitude with $|\Delta\ell| = 2\ell$ [14], and $c_j (j = 1, 2, 3)$ is also crosstalk amplitude but $|\Delta\ell| = 1$ [24],

$$a = |\langle\psi_{\pm\ell}|\pm\ell\rangle|^2 = \frac{1}{2\pi}\int_0^\infty r\left|R_{\ell,p}(r)\right|^2 \mathrm{d}r \int_0^{2\pi} \mathrm{d}\theta \exp[-0.5D_\phi(2r|\sin(\theta/2)|)], \quad (20)$$

$$b = |\langle\psi_{\pm\ell}|\mp\ell\rangle|^2 = \frac{1}{2\pi}\int_0^\infty r\left|R_{\ell,p}(r)\right|^2 \mathrm{d}r \int_0^{2\pi} \mathrm{d}\theta \exp(-2\mathrm{i}\ell\theta) \exp[-0.5D_\phi(2r|\sin(\theta/2)|)], \quad (21)$$

$$c_1 = |\langle\psi_{\pm\ell}|\pm\ell\pm1\rangle|^2 = \frac{1}{2\pi}\int_0^\infty r\left|R_{\ell,p}(r)\right|^2 \mathrm{d}r \int_0^{2\pi} \mathrm{d}\theta \exp(-\mathrm{i}\theta) \exp[-0.5D_\phi(2r|\sin(\theta/2)|)], \quad (22)$$

$$c_2 = |\langle\psi_{\pm\ell\pm1}|\pm\ell\rangle|^2 = \frac{1}{2\pi}\int_0^\infty r\left|R_{\pm\ell\pm1,p}(r)\right|^2 \mathrm{d}r \int_0^{2\pi} \mathrm{d}\theta \exp(-\mathrm{i}\theta) \exp[-0.5D_\phi(2r|\sin(\theta/2)|)], \quad (23)$$

$$c_3 = |\langle\psi_{\pm\ell\mp1}|\pm\ell\rangle|^2 = \frac{1}{2\pi}\int_0^\infty r\left|R_{\pm\ell\mp1,p}(r)\right|^2 \mathrm{d}r \int_0^{2\pi} \mathrm{d}\theta \exp(-\mathrm{i}\theta) \exp[-0.5D_\phi(2r|\sin(\theta/2)|)]. \quad (24)$$

Here we use the non-Kolmogorov power spectrum for the investigation of the evolution of OAM entanglement in turbulence. The non-Kolmogorov power spectrum for the refractive index fluctuations is given by [29,30]

$$\Phi_n(\kappa,\alpha) = A(\alpha)\widetilde{C}_n^2(\kappa^2+\kappa_0^2)^{-\alpha/2}\exp(-\kappa^2/\kappa_m^2), \quad 3<\alpha<4, \quad (25)$$

α being the generalized exponent, $\widetilde{C}_n^2$ (in units of $\mathrm{m}^{\alpha-3}$) being a generalized refractive-index structure parameter, $\kappa_0 = 2\pi/L_0$, L_0 representing the outer scale of turbulence, $\kappa_m = c(\alpha)/l_0$, l_0 representing the inner scale of turbulence, and κ being the magnitude of the three-dimensional wave number vector, and

$$c(\alpha) = (\Gamma(5-\alpha/2)A(\alpha)2\pi/3)^{\frac{1}{\alpha-5}}, \quad (26)$$

$$A(\alpha) = 1/4\pi^2\Gamma(\alpha-1)\cos(\alpha\pi/2), \quad (27)$$

where $\Gamma(x)$ is the gamma function of the term. When $\alpha = 11/3$, $L_0 = \infty$, $l_0 = 0$, and $\widetilde{C}_n^2 = C_n^2$, Equation (25) can be reduced to the conventional Kolmogorov spectrum [29]

$$\Phi_n(\kappa) = 0.033C_n^2\kappa^{-11/3}. \quad (28)$$

$D_\phi(r)$ is a two-point spherical wave structure function that contains the influence of atmospheric turbulence, which can be expressed as [31,32]

$$D_\phi(\mathbf{r}_1,\mathbf{r}_2;z) = 8\pi^2k^2z\int_0^1 \mathrm{d}\varsigma\int_0^\infty \{1-J_0[\kappa|\varsigma(\mathbf{r}_1-\mathbf{r}_2)|]\}\Phi_n(\kappa,\alpha)\kappa\mathrm{d}\kappa, \quad (29)$$

where ς denotes the normalized distance variable, $J_0(\cdot)$ is the zero-order Bessel function of the first kind and has the approximation

$$J_0(\kappa|\varsigma(\mathbf{r}_1-\mathbf{r}_2)|) = 1-\frac{1}{4}(\kappa|\varsigma(\mathbf{r}_1-\mathbf{r}_2)|)^2. \quad (30)$$

Under the quadratic approximation of Rytov's phase structure function [32–35], the term $\exp[-0.5D_\phi(2r|\sin(\theta/2)|)]$ can be written as

$$\exp[-0.5D_\phi(2r|\sin(\theta/2)|)] = \exp\left[-(2r|\sin(\theta/2)|/\rho_0)^2\right], \quad (31)$$

where ρ_0 is the spatial coherence length of a spherical wave propagating in a non-Kolmogorov turbulent atmosphere, and [32]

$$\rho_0 = \left(\frac{\pi^2k^2zA(\alpha)}{6(\alpha-2)}\widetilde{C}_n^2[\kappa_m^{2-\alpha}\exp(\frac{\kappa_0^2}{\kappa_m^2})\left(2\kappa_0^2-2\kappa_m^2+\alpha\kappa_m^2\right)\Gamma(2-\frac{\alpha}{2},\frac{\kappa_0^2}{\kappa_m^2})-2\kappa_0^{4-\alpha}]\right)^{-1/2}. \quad (32)$$

The propagation of the states $|\ell\rangle(|-\ell\rangle)$ and $|\pm\ell\pm1\rangle(|\pm\ell\mp1\rangle)$ through atmospheric turbulence change into the states $|\psi_\ell\rangle(|\psi_{-\ell}\rangle)$ and $|\psi_{\pm\ell\pm1}\rangle(|\psi_{\pm\ell\mp1}\rangle)$, respectively.

Wootter's concurrence is used to evaluate the entanglement degree of the output bipartite OAM state [25], which is given by

$$C(\rho) = \max\{0, \lambda_1 - \lambda_2 - \lambda_3 - \lambda_4\}, \tag{33}$$

where λ_i are the eigenvalues of the Hermitian matrix ξ, which are ranked by decreasing order, and

$$\xi = \rho_{\text{out}}(\sigma_y \otimes \sigma_y)\rho^*_{\text{out}}(\sigma_y \otimes \sigma_y), \tag{34}$$

Asterisk (*) indicating the conjugate of a complex number, σ_y given by

$$\sigma_y = \begin{pmatrix} 0 & -\mathrm{i} \\ \mathrm{i} & 0 \end{pmatrix}. \tag{35}$$

3. Numerical Results and Analysis

Firstly, our results of numerical evaluation are compared with the results based on S&R theory [9]. The turbulence parameters are set to be $\alpha = 11/3$, L_0= 500 m, and l_0= 1 mm. As shown in Figure 2, the results of numerical evaluation agree with S&R theory well when $|\ell| \leq 3$ and p= 0. In other cases, the results of numerical evaluation deviate significantly from the result in S&R theory. Consequently, the effect of backward scattering can be ignored when OAM is in lower-order mode, but it is very crucial for higher-order OAM entanglement.

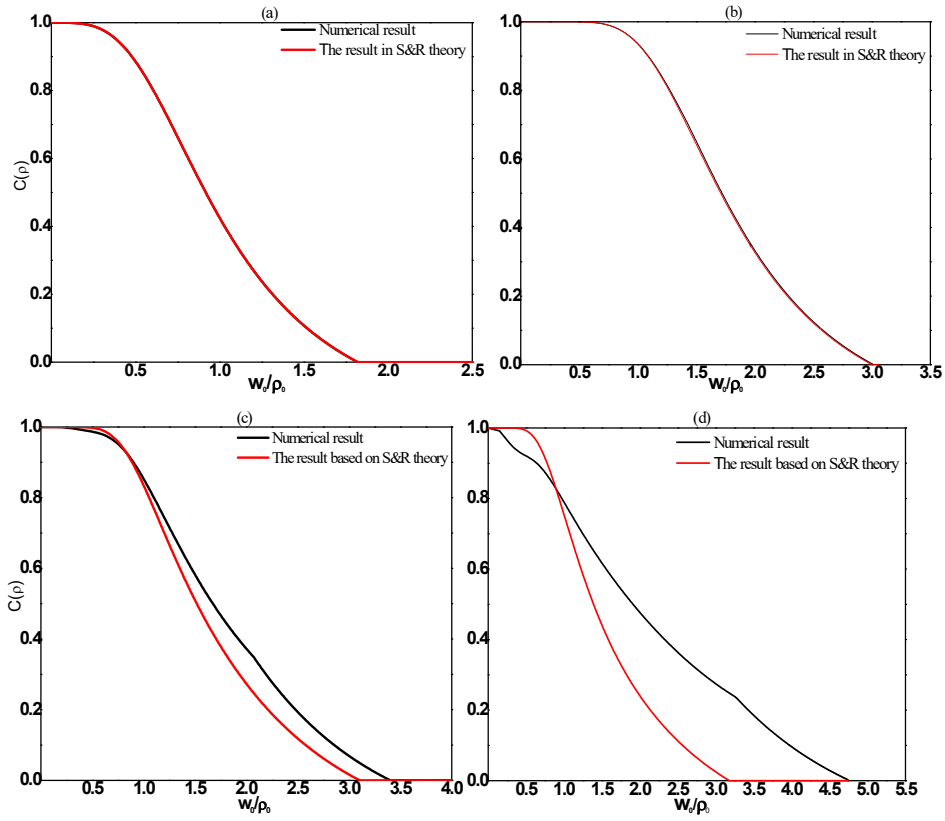

Figure 2. Concurrence plotted as a function of ratio w_0/ρ_0(the turbulence strength) for different OAM modes. In (**a**) $\ell = 1, p = 0$, in (**b**) $\ell = 3, p = 0$, in (**c**) $\ell = 3, p = 1$, in (**d**) $\ell = 3, p = 2$.

Now the entanglement evolution of the higher-order OAM entangled state in non-Kolmogorov weak turbulence is investigated. In the following numerical examples, the beam parameters are set to be ℓ= 3, p = 2, w_0 = 0.08 m, and λ = 1064 nm, and the parameters of turbulence are set to be α= 3.6, L_0= 10 m, l_0 = 1mm, and $\widetilde{C}_n^2$= 8×10^{-14} $\mathrm{m}^{3-\alpha}$, unless otherwise specified. The results of the numerical evaluation are presented in Figures 3–6.

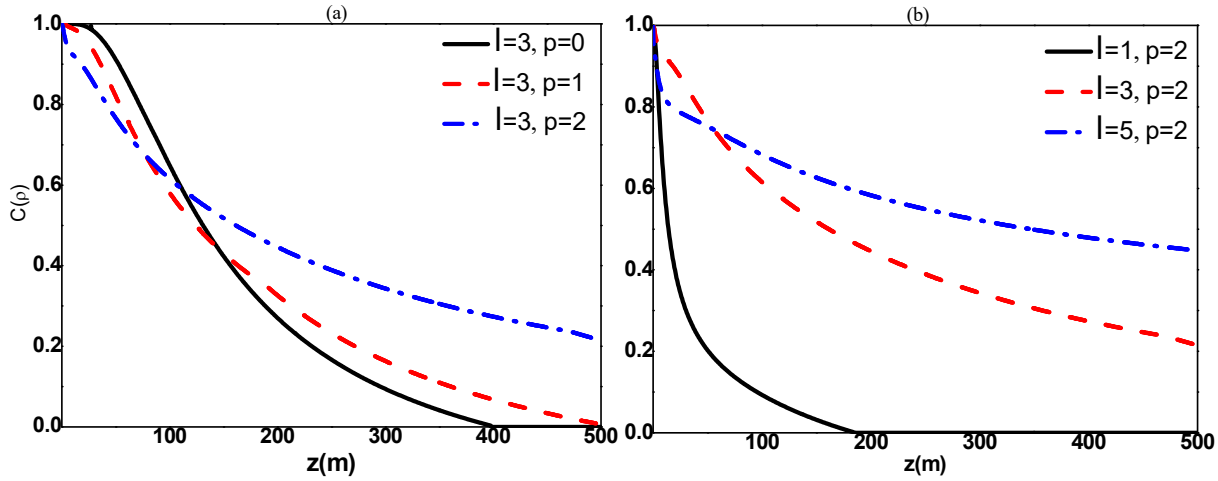

Figure 3. Concurrence versus propagation distance for different beam parameters. (**a**) For the different values of radial quantum number and (**b**) for the different values of azimuthal mode order.

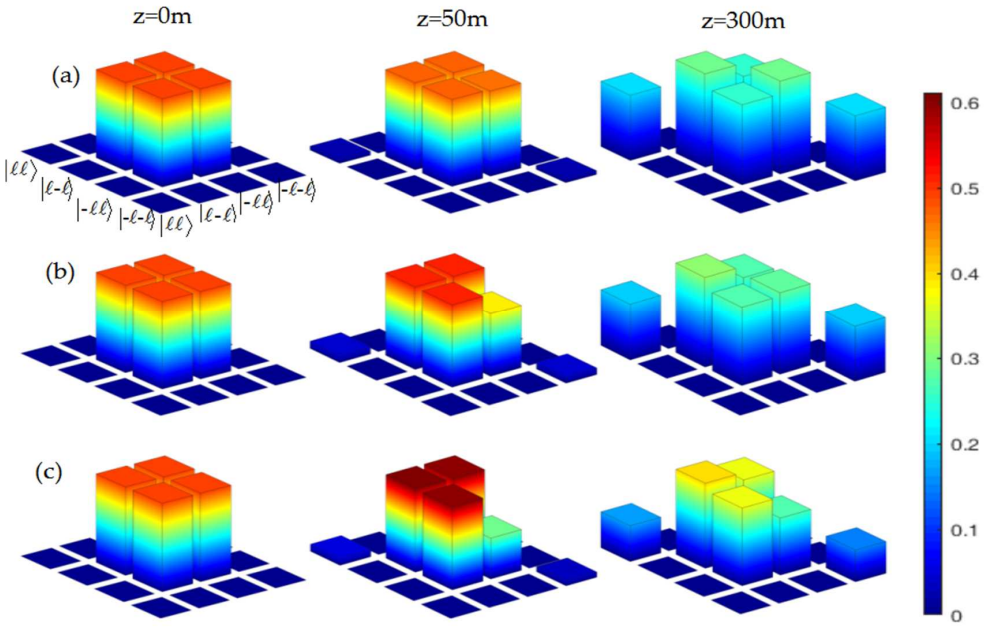

Figure 4. Graphic representations of the density matrices.The diagonal elements of the density matrices are horizontally arranged. (**a**) for $\ell = 3$, $p = 0$; (**b**) for $\ell = 3$, $p = 1$; (**c**) for $\ell = 3$, $p = 2$.

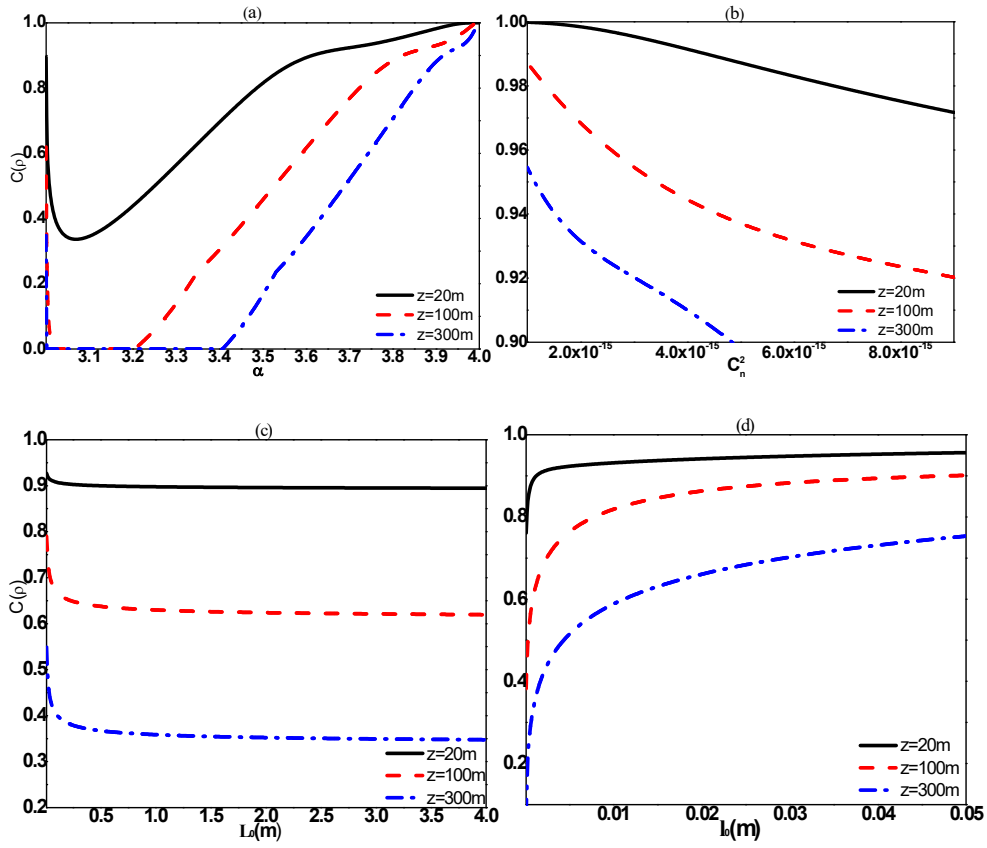

Figure 5. Concurrence plotted as the turbulence parameters for different propagation distances (**a**) of generalized exponent, (**b**) of refractive-index structure parameter, (**c**) of turbulence outer scale, and (**d**) of turbulence inner scale.

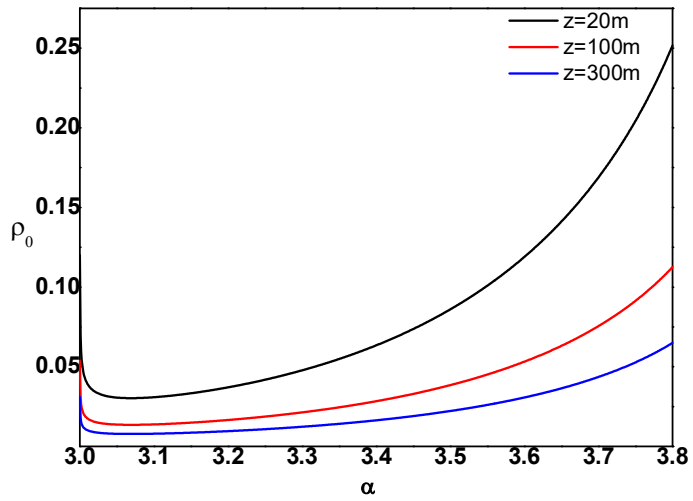

Figure 6. The spatial coherence length plotted as a function of α for different propagation distances.

Figure 3 shows the concurrence versus the propagation distance z for different beam parameters. As shown in Figure 3a,b, the concurrence lasts longer for higher value of the azimuthal mode and larger radial quantum number. Moreover, one observes that when the entangled photon propagates only a relatively short distance within 100 m, the concurrence decays quickly for larger radial quantum number, shown in Figure 3a. Such results can be interpreted as follows. As shown in Figure 4, the density matrices for a pair of entangled qutrits are 4×4 matrices. For z = 0 m, the magnitudes of the central density elements are all 0.5, and the input states have the highest purity. The same heights

(magnitudes of the elements) indicate that the input state is maximally entangled [21]. For z = 50 m, the central elements in the density matrix vary more significantly as the value of radial quantum number increases, meaning that the purity decreases quickly for OAM entanglement with the radial quantum number increasing. When the propagation distance is 300 m, the diagonal elements in the density matrix grow more rapidly at the cost of the central density elements that represent the original input state [21]. However, the diagonal elements dominate over the other elements more slowly as the value of the radial quantum number increases, meaning that OAM entanglement with higher radial quantum number is more robust. These results also reflect the fact that scattering from one OAM state to another depends not only on the change in OAM ($\Delta\ell$) [9], but also on different radial intensity profiles $R_{\ell,p}(r,z)$.

Figure 5 presents the dependence of the concurrence on turbulence parameters for different propagation distances. From Figure 5a, it can be seen that as the generalized exponent increases, the concurrence drops off sharply to a minimum value at about 3.07, and then gradually increases to the maximum value. In addition, when α reaches around 3.07, OAM entanglement gradually decreases to zero for z $\geq$ 100 m. Such a phenomenon suggests that the condition of turbulence with the generalized exponent around α= 3.07 is not suitable for OAM entanglement transmission. This can be understood as follows: as shown in Figure 6, the spatial coherence length ρ_0 first decreases as α increases, reaches a minimum value when α is about 3.07, and then increases with further increase of α. The LG beam suffers the most serious perturbation when α is about 3.07 [28]. As a result, the influence of turbulence on the OAM entanglement is the most serious near α=3.07. Figure 5b demonstrates the fact that the OAM entanglement always decays in the weak turbulence, but the rate of decay becomes very slow when the value of the refractive-index structure parameter decreases. That is, the entanglement evolution of the OAM state will be impacted less by turbulence with a smaller refractive-index structure parameter. Figure 5c denotes that the concurrence lasts longer for a smaller value of the turbulence outer scale, revealing that the entanglement evolution of the OAM state will be impacted more severely by turbulence with a larger outer scale. It can also be seen that under the condition $L_0 \geq$ 1m, the influence of outer scale on the entanglement evolution of the OAM state is very slight. In Figure 5d, it can be found that the concurrence can survive over a longer distance with increasing turbulence inner scale. This means that turbulence with a lager inner scale has less influence on the OAM entanglement.

4. Discussion and Conclusions

In this paper, the entanglement evolution of OAM photons with higher-order OAM mode propagating across a non-Kolmogorov turbulent atmosphere has been numerically evaluated. Here, we only considered the case that two photons both have passed through turbulence. The expression for the output density matrix of entangled photons with higher-order OAM mode has been obtained. In contrast with the result based on S&R theory, the output density matrix takes into account the effect of backward scattering. The results of numerical evaluation show that the effect of backward scattering can be ignored for OAM entanglement in lower-order mode, while it is very crucial for higher-order mode OAM entanglement.

Quadratic approximation of the non-Kolmogorov phase structure function is used to estimate the evolution of OAM entanglement. When the non-Kolmogorov power spectrum is reduced to the Kolmogorov spectrum and the effect of backward scattering can be ignored, our numerical results are consistent with the results reported by Bachmann et al [36], who analyzed the universal entanglement decay laws for the quadratic approximation.

There are various aspects that pose challenges to experimental work on the propagation of entangled photons with higher-order OAM mode entangled states through turbulence. In practical scenarios it is more difficult and complex to produce entangled photon pairs with larger radial quantum number. In addition, it is also observed that modes with higher value of the azimuthal mode are more difficult to measure experimentally. Therefore, more work remains to be done in the future.

In summary, the decay of entangled orbital angular momentum (OAM) photons propagating across non-Kolmogorov turbulence has been investigated. In this work, we explore the evolution of OAM entanglement in the weak scintillation regime and consider the effect of backward scattering on OAM entanglement with higher-order OAM mode. The results of the numerical evaluation reveal that the concurrence monotonically decreases in turbulence, but the OAM entangled state with higher value of the azimuthal mode and larger radial quantum number lasts much longer, which means OAM entangled states with higher value of the azimuthal mode and larger radial quantum number are more appropriate to quantum communication over long distances. Meanwhile, non-Kolmogorov turbulence with a smaller refractive-index structure parameter, a smaller turbulence outer scale or a larger turbulence inner scale affects OAM entanglement evolution less. In addition, the influence of turbulence on the entanglement evolution of the OAM state is the most serious when the generalized exponent is around 3.07, and thus the condition of turbulence with the generalized exponent around 3.07 is not suitable for OAM entanglement transmission. Our findings will be very important to improve the performance of a free-space quantum communication system.

Author Contributions: Conceptualization, X.Y. and B.W.; methodology, P.Z.; validation, J.Z. and X.Y.; formal analysis, B.W.; investigation, P.Z. and J.Z.; writing—original draft preparation, X.Y. and P.Z.; writing—review and editing, B.W.; project administration, J.Z.; funding acquisition, B.W.; Funding acquisition, X.Y. All authors have read and agreed to the published version of the manuscript.

Funding: This work was supported by the Project of the Hubei Provincial Department of Education (Grant No. B2019148) and the National Natural Science Foundation of China (Grant No. 11847118).

Institutional Review Board Statement: Not applicable.

Informed Consent Statement: Not applicable.

Conflicts of Interest: None of the authors have any proprietary or financial interest in any of the materials or methods discussed.

References

1. Ren, Y.; Wang, Z.; Liao, P.; Li, L.; Xie, G.; Huang, H.; Zhao, Z.; Yan, Y.; Ahmed, N.; Willner, A.; et al. Experimental characterization of a 400 Gbit/s orbital angular momentum multiplexed free-space optical link over 120 m. *Opt. Lett.* **2016**, *41*, 622. [CrossRef] [PubMed]
2. Leach, J.; Bolduc, E.; Gauthier, D.J.; Boyd, R.W. Secure information capacity of photons entangled in many dimensions. *Phys. Rev. A* **2012**, *85*, 060304. [CrossRef]
3. Wang, A.; Zhu, L.; Wang, L.; Ai, J.; Chen, S.; Wang, J. Directly using 8.8-km conventional multi-mode fiber for 6-mode orbital angular momentum multiplexing transmission. *Opt. Express* **2018**, *26*, 10038. [CrossRef] [PubMed]
4. Trichili, A.; Salem, A.B.; Dudley, A.; Zghal, M.; Forbes, A. Encoding information using Laguerre Gaussian modes over free space turbulence media. *Opt. Lett.* **2016**, *41*, 3086. [PubMed]
5. Zhu, L.; Liu, J.; Mo, Q.; Du, C.; Wang, J. Encoding/decoding using superpositions of spatial modes for image transfer in km-scale few-mode fiber. *Opt. Express* **2016**, *24*, 16934. [CrossRef]
6. Groblacher, S.; Jennewein, T.; Vaziri, A.; Weihs, G.; Zeilinger, A. Experimental quantum cryptography with qutrits. *New J. Phys.* **2006**, *8*, 75. [CrossRef]
7. Jeong, H.; Kim, M.S. Efficient quantum computation using coherent states. *Phys. Rev. A* **2002**, *65*, 042305. [CrossRef]
8. Ralph, T.C.; Gilchrist, A.; Milburn, G.J. Quantum computation with optical coherent states. *Phys. Rev. A* **2003**, *68*, 042319.
9. Smith, B.J.; Raymer, M.G. Two-photon wave mechanics. *Phys. Rev. A* **2006**, *74*, 062104. [CrossRef]
10. Jha, A.K.; Tyler, G.A.; Boyd, R.W. Effects of atmospheric turbulence on the entanglement of spatial two-qubit states. *Phys. Rev. A* **2010**, *81*, 1532.
11. Roux, F.S. Infinitesimal-propagation equation for decoherence of an orbital-angular-momentum-entangled biphoton state in atmospheric turbulence. *Phys. Rev. A* **2011**, *83*, 053822. [CrossRef]
12. Sheng, X.; Zhang, Y.; Zhao, F.; Zhang, L.; Zhu, Y. Effects of low-order atmosphere-turbulence aberrations on the entangled orbital angular momentum state. *Opt. Lett.* **2012**, *37*, 2607. [CrossRef] [PubMed]
13. Gonzalez Alonso, J.R.; Brun, T.A. Protecting orbital-angular momentum photons from decoherence in turbulent atmosphere. *Phys. Rev. A* **2013**, *88*, 022326. [CrossRef]
14. Leonhard, N.D.; Shatokhin, V.N.; Buchleitner, A. Universal entanglement decay of photonic-orbital-angular-momentum qubit states in atmospheric turbulence. *Phys. Rev. A* **2015**, *91*, 012345. [CrossRef]

15. Ibrahim, A.H.; Roux, F.S.; McLaren, M.; Konrad, T.; Forbes, A. Orbital-angular-momentum entanglement in turbulence. *Phys. Rev. A* **2013**, *88*, 012312. [CrossRef]
16. Ibrahim, A.H.; Roux, F.S.; Konrad, T. Parameter dependence in the atmospheric decoherence of modally entangled photon pairs. *Phys. Rev. A* **2014**, *90*, 052115. [CrossRef]
17. Yan, X.; Zhang, P.F.; Zhang, J.H.; Qiao, C.H.; Fan, C.Y. Decoherence of orbital angular momentum photons tangled in non-Kolmogorov turbulence. *J. Opt. Soc. Am. A* **2016**, *33*, 1831. [CrossRef]
18. Yan, X.; Zhang, P.F.; Zhang, J.H.; Feng, X.X.; Qiao, C.H.; Fan, C.Y. Effect of atmospheric turbulence on entangled orbital angular momentum three-qubit state. *Chin. Phys. B* **2017**, *26*, 064202. [CrossRef]
19. Zhang, L.; Zhu, Y. The influence of non-Kolmogorov turbulence on the entanglement of spatial two-qubit states in a slant channel. *Optik* **2014**, *125*, 1259–1263. [CrossRef]
20. Brunner, T.; Roux, F.S. Robust entangled qutrit states in atmospheric turbulence. *New J. Phys.* **2013**, *15*, 063005. [CrossRef]
21. Zhang, Y.W.; Prabhakar, S.; Ibrahim, A.H.; Roux, F.S.; Forbes, A.; Konrad, T. Experimentally observed decay of high-dimensional entanglement through turbulence. *Phys. Rev. A* **2016**, *94*, 032310. [CrossRef]
22. Paterson, C. Atmospheric Turbulence and Orbital Angular Momentum of Single Photons for Optical Communication. *Phys. Rev. Lett.* **2005**, *94*, 153901. [CrossRef] [PubMed]
23. Sorelli, G.; Shatokhin, V.N.; Roux, F.S.; Buchleitner, A. Entanglement of truncated quantum states. *Quantum Sci. Technol.* **2020**, *5*, 035012. [CrossRef]
24. Yan, X.; Zhang, P.F.; Fan, C.Y.; Zhang, J.H. Effect of atmospheric turbulence on orbital angular momentum entangled state. *Commun. Theor. Phys.* **2022**, *74*, 025102. [CrossRef]
25. Wootters, W.K. Entanglement of formation of an arbitrary state of two qubits. *Phys. Rev. Lett.* **1998**, *80*, 2245–2248. [CrossRef]
26. Allen, L.; Beijersbergen, M.W.; Spreeuw RJ, C.; Woerdman, J.P. Orbital angular momentum of light and the transformation of Laguerre-Gaussian laser modes. *Phys. Rev. A* **1992**, *45*, 8185–8189. [CrossRef]
27. Beijersbergen, M.W.; Allen, L.; Van Der Veen, H.E.L.O.; Woerdman, J.P. Astigmatic laser mode converters and transfer of orbital angular momentum. *Opt. Commun.* **1993**, *96*, 123–132. [CrossRef]
28. Zeng, J.; Liu, X.L.; Zhao, C.L.; Wang, F.; Gbur, G.; Cai, Y.J. Spiral spectrum of a Laguerre-Gaussian beam propagating in anisotropic non-Kolmogorov turbulent atmosphere along horizontal path. *Opt. Express* **2019**, *27*, 25342. [CrossRef]
29. Toselli, I.; Andrews, L.C.; Phillips, R.L.; Ferrero, V. Free-space optical system performance for laser beam propagation through non-kolmogorov turbulence. *Opt. Eng.* **2007**, *47*, 026003.
30. Stribling, B.E.; Welsh, B.M.; Roggemann, M.C. Optical propagation in non-Kolmogorov atmospheric turbulence. In Proceedings of the SPIE's 1995 Symposium on OE/Aerospace Sensing and Dual Use Photonics, Orlando, FL, USA, 15 June 1995; Volume 2471, pp. 181–196.
31. Zhao, L.; Xu, Y.; Yang, S. Statistical properties of partially coherent vector beams propagating through anisotropic atmospheric turbulence. *Optik* **2021**, *227*, 166115. [CrossRef]
32. Xu, H.F.; Cui, Z.F.; Qu, J. Propagation of elegant Laguerre-Gaussian beam in non-Kolmogorov turbulence. *Opt. Express* **2011**, *19*, 211. [CrossRef] [PubMed]
33. Shirai, T.; Dogariu, A.; Wolf, E. Directionality of Gaussian Schell-model beams propagating in atmospheric turbulence. *Opt. Lett.* **2003**, *28*, 610. [CrossRef] [PubMed]
34. Shchepakina, E.; Korotkova, O. Second-order statistics of stochastic electromagnetic beams propagating through non-Kolmogorov turbulence. *Opt. Express* **2010**, *18*, 10650. [CrossRef] [PubMed]
35. Zhou, P.; Ma, Y.; Wang, X. Average spreading of a Gaussian beam array in non-Kolmogorov turbulence. *Opt. Lett.* **2010**, *35*, 1043. [CrossRef] [PubMed]
36. Bachmann, D.; Shatokhin, V.N.; Buchleitner, A. Universal entanglement decay of photonic orbital angular momentum qubit states in atmospheric turbulence: An analytical treatment. *J. Phys. A Math. Theor.* **2019**, *52*, 405303. [CrossRef]